Journal of Power Sources 366 (2017) 65–71

Contents lists available at ScienceDirect

Journal of Power Sources

journal homepage: www.elsevier.com/locate/jpowsour

On-site chemical pre-lithiation of S cathode at room temperature on a 3D nano-structured current collector

Yunwen Wu [a], Toshiyuki Momma [a, b, *], Seongki Ahn [b], Tokihiko Yokoshima [b], Hiroki Nara [b], Tetsuya Osaka [a, b]

[a] Graduate School of Advanced Science and Engineering, Waseda University, 3-4-1, Okubo, Shinjuku-ku, Tokyo 169-8555, Japan
[b] Research Organization for Nano and Life Innovation, Waseda University, 513, Wasedatsurumakicho, Shinjuku-ku, Tokyo 162-0041, Japan

HIGHLIGHTS

- A chemical pre-lithiation method was proposed to pre-lithiate S cathode.
- Room temperature pre-lithiation was realized by using 3D current collector.
- Pre-lithiated S cathode made in room temperature showed improved performance.
- The reaction is conducted by a simple on-site drop process on the S cathode.

GRAPHICAL ABSTRACT

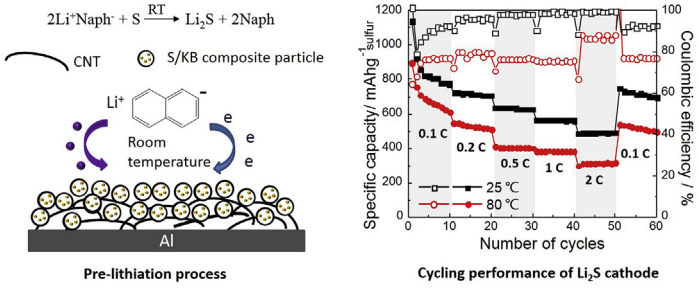

ARTICLE INFO

Article history:
Received 25 May 2017
Received in revised form
13 August 2017
Accepted 30 August 2017

Keywords:
Pre-lithiation
Li-S battery
CNT
Room temperature
Lithium naphthalenide

ABSTRACT

This work reports a new chemical pre-lithiation method to fabricate lithium sulfide (Li_2S) cathode. This pre-lithiation process is taken place simply by dropping the organolithium reagent lithium naphthalenide (Li^+Naph^-) on the prepared sulfur cathode. It is the first time realizing the room temperature chemical pre-lithaition reaction attributed by the 3D nanostructured carbon nanotube (CNT) current collector. It is confirmed that the Li_2S cathode fabricated at room temperature showing higher capacity and lower hysteresis than the Li_2S cathode fabricated at high temperature pre-lithiation. The pre-lithiated Li_2S cathode at room temperature shows stable cycling performance with a 600 mAh g^{-1} capacity after 100 cycles at 0.1 C-rate and high capacity of 500 mAh g^{-1} at 2 C-rate. This simple on-site pre-lithiation method at room temperature is demonstrated to be applicable for the in-situ pre-lithiation in a Li metal free battery.

1. Introduction

Recent years, the rechargeable Li^+ ion batteries become an important power source for stationary energy storage, electric vehicles and portable electronics. However, the current rechargeable batteries still cannot satisfy the commercial use in electric vehicles [1,2]. Sulfur, with a high theoretical specific capacity of 1672 mAh g^{-1} is a promising cathode candidate for the next generation of high capacity rechargeable batteries [3]. Much efforts have been exerted on conquering the insulate nature of sulfur and the shuttle effect to improve the cycling performance [4–8]. However, the Li metal was usually used as anode because of the lack of Li^+ ion source in the S cathode. In order to meet the practical

* Corresponding author. Graduate School of Advanced Science and Engineering, Waseda University, 3-4-1, Okubo, Shinjuku-ku, Tokyo 169-8555, Japan.
E-mail address: momma@waseda.jp (T. Momma).

http://dx.doi.org/10.1016/j.jpowsour.2017.08.113

application, the safety issues caused by the Li dendrite formed in the Li metal anode have to be seriously considered.

Lithium sulfide (Li_2S) as a Li^+ ion rich S base cathode material, which has the ability to pair with the Li metal free anodes, is thought to be the solution for relieving the safety problem [9–12]. Li_2S has high theoretical capacity about 1162 mAh g^{-1} with the Li^+ ion intercalation and de-intercalation process of $8Li_2S \leftrightarrow S_8 + 16Li^+ + 16e^-$ [13]. However, its insulating nature and polysulfide dissolution still hinder its electrochemical performance. In addition, Li_2S cathode showed huge over potential barrier in the first charge curve because of its insulating nature [14,15]. The normal way used for S cathode by heat melting process at 155 °C [5] is not workable for Li_2S cathode fabrication because of the high melting temperature of Li_2S. In this situation, most researchers focused on reducing the Li_2S particle size to improve the contacting surface area with conductive materials (mostly carbon materials) to increase the electronic conductivity of Li_2S cathode. In 2012, it was first reported that by ball milling commercial Li_2S powder to get micro-sized Li_2S, low C-rate performance was realized [16]. By ball milling method of the commercial Li_2S powder, it is difficult to get the nano-sized Li_2S material [17,18]. Recrystallization of Li_2S solution is another way to fabricate Li_2S micro-nano sized particles from commercial Li_2S powder [19–21]. Graphene has been used as a conductive Li_2S holder to recrystallize Li_2S nanoparticles [20,22]. Though boosted electrochemical performance has been obtained by nano sizing the commercial Li_2S powder, these methods are time consuming and staying in the laboratory reaction scale. Recently, the high temperature reducing reaction has been used to fabricate Li_2S particles with a micro-nano size [23–26]. N-butyllithium as a normal organolithium reagent has been used to react with sulfur to fabricate Li_2S nanoparticles at a high temperature about 100 °C [27–30]. However, the extremely high reaction temperature at a Ar atmosphere greatly increase the production cost. As a result, it is important to develop a convenient way to fabricate the Li_2S cathode with good performance for the future development of Li metal free sulfur full cell.

In this study, we reported a chemical pre-lithiation method to fabricate Li_2S mesoporous carbon composite cathode at room temperature on a 3D nanostructured multi-wall carbon nano tubes (CNT) support. The reaction occurs on the sulfur nano carbon (Ketjenblack, KB) composite cathode, the amorphous state sulfur can be reduced to Li_2S directly by dropping lithium naphthalenide (Li^+Naph^-). The 3D nanostructured CNT layer provides more diffusion path for Li^+Naph^- to react completely with S at room temperature. The electrochemical performance of the fabricated Li_2S/KB composite cathode on CNT (denoted as Li_2S/KB/CNT cathode) was analyzed to demonstrate the outstanding cycling behavior at different C-rates.

2. Experimental

2.1. Preparation

2.1.1. Preparation of S/KB composite cathode

The S/KB composite was prepared by mixing S powder (Sigma-Aldrich) with KB in a 1:1 weight ratio using a granulator (Balance Gran, AKIRAKIKO). The mixture was then heated in an Ar atmosphere at a temperature of 155 °C for 12 h to form a composite of S and KB. The S/KB composite slurry was prepared in the granulator. The S/KB slurry was made by mixing the S/KB composite and polyvinylidene difluoride (PVdF) binder (Sigma-Aldrich) with a weight ratio of 9:1 in N-methylpyrrolidone (NMP), which acted as the solvent. In order to prepare the S/KB composite cathode, the slurry was applied to the current collector substrate using the doctor blade method and dried for 24 h in a dry atmosphere (at the dew point of below −40 °C, RT).

2.1.2. Electrophoretic deposition of CNT [31]

The CNT/Al substrate was fabricated by electrophoretic deposition. Commercial thin multi-walled CNT (NC7000), which has carbon purity around 90% with diameter around 10 nm, were purchased from nanocyl. As-received CNT were oxidized in concentrated H_2SO_4/HNO_3 (3:1; v/v, 96.0% and 60.0%, respectively) for 4 h at 45 °C by sonication to functionalize surface of CNT, and washed until pH 7. After washing process, the oxidized CNT were dried in vacuum oven at 80 °C for 4 h. The oxidized CNT (0.05 mg mL^{-1}) and cobalt dichloride ($CoCl_2$) (0.5 mg mL^{-1}) are sonicated in isopropyl alcohol (IPA) for 30 min by sonication, separately, followed by both of dispersed samples were sonicated together in same bottle for 30 min again. The Co^{2+} ion is used to bond with the negatively charged CNT, forming Co(CNT)/Al to provide high electrostatic repulsion force for deposition. The Al substrates with an exposed area of 1×1 cm^{-2} and a gap of 0.7 cm were soaked in CNT and $CoCl_2$ suspension with glass cell. A direct current power supply was used as power resource with a voltage of −120 V for 5 min. After that, prepared CNT/Al substrate was washed with distilled water and ethanol to remove aggregated CNT particles and impurities of their surface. Afterward, the CNTs/Al substrate was dried at room temperature for overnight.

2.1.3. Fabrication of Li^+Naph^- solution

As Li metal and Li_2S are both sensitive to moisture in air, all the following synthesis work was carried out in an argon filled glove box with a moisture content below 0.1 ppm and oxygen levels below 5 ppm. The Li^+Naph^- was prepared by mixing equal mol amount of Li metal and naphthalene (Naph) in tetrahydrofuran (THF) to fabricate 1 M Li^+Naph^- solution. After stirring for 3 h at room temperature, the solution turned into dark green, indicating the totally fabrication of Li^+Naph^- in THF [32].

2.1.4. Fabrication of Li_2S cathode

The 1M Li^+Naph^- THF solution was dropped on S/KB cathode. The molar ratio of the Li^+Naph^- and S was Li^+Naph^-: S was 2:1. After 10 min reaction, the cathode was rinsed by THF solution to remove the residues of reagents. Then the sample was dried in the glovebox for 20 min.

2.2. Characterization

Scanning electron microscopy (SEM) images were obtained by field emission SEM (FE-SEM, S-4500S, Hitachi). The crystalline structure of the Li_2S powder was obtained by X-ray diffraction (XRD, Rigaku, RINT-Ultima III) with the protection of a Kapton tape. The composite of the cathode was characterized by means of field emission scanning electron microscopy with an energy dispersive X-ray analyzer (FESEM-EDX, Hitachi, S-4800) and X-ray photoelectron spectroscopy (XPS, JEOL, JPS-9010TR).

2.3. Electrochemical measurement

Coin type 2032 cells were assembled in an Ar filled glove box. The electrolyte was composed of 1.0 M lithium bis(trifluoromethanesulfonyl)imide (LiTFSI) in dioxolane (DOL)/Dimethoxyethane (DME) (1:1 vol ratio) with 1 wt% lithium nitrate ($LiNO_3$) as addictive. 25 μm thick polypropylene porous film as the separator, Li metal foil as the anode in the half cell. The galvanostatic charge discharge tests were conducted using a charge discharge system (TOSCAT-3100, Toyo system) at different C-rates from 0.1 C-rate to 2 C-rate between 1.8 and 2.6 V. Cyclic voltammetry (CV) with a scan rate of 0.1 mV s^{-1} was conducted using

electrochemical measurement equipment (HZ-5000, Hokuto Denko).

3. Results and discussion

Lithium naphthalenide (Li^+Naph^-), with a two conjugate benzene rings is a relative moderate organolithium reducing reagent [33]. It is innovatively employed to react with sulfur cathode to fabricate Li_2S cathode by a simple drop process. The overall reaction is supposed to be:

$$2Li^+Naph^- + S \rightarrow Li_2S + 2Naph \quad (1)$$

Fig. 1a illustrated the fabrication method of the Li_2S/KB/CNT cathode. At first, the CNT layer was deposited on Al foil by electrophoretic deposition [31]. The morphology of the deposited highly porous 3D nanostructured multi-wall CNT with a diameter about 23 nm is showed in Fig. 1b. After the CNT/Al sheet was dried for one day, the S/KB composite slurry was coated on the CNT layer. The surface morphology is observed by SEM showed in Fig. 1c. The uniform distributed S/KB nanoparticles with a diameter of 50 nm can be observed by SEM analysis after totally dried showing in Fig. 1c. This S/KB composite on a CNT/Al substrate is denoted as S/KB/CNT electrode. For the process of chemical pre-lithiation, a calculated amount of the synthesized 1 M Li^+Naph^- solution in THF was dropped on the S/KB/CNT electrode to make the fully lithiation reaction. After 10 min reaction, the electrode was rinsed by THF solution to remove the side products (mainly Naph). This product was denoted as Li_2S/KB/CNT electrode after it was dried in glovebox. The surface of the Li_2S/KB/CNT cathode showed relative smooth morphology, from which the S/KB nanoparticles still can be distinguished in the SEM image showed in Fig. 1d. This indicates the fabricated Li_2S/KB/CNT cathode still keeps the structure of S/KB nanocomposites with a certain degree of volume expansion.

XRD analysis has been used to test the S/KB composite thin film in S/KB/CNT cathode before and after lithiation. Since no crystalline peaks related to sulfur can be observed in the S/KB cathode due to its low crystallinity structure [34]. We did chemical reaction experiment by adding sulfur powder into Li^+Naph^- THF solution to verify the reaction product. After 4 h stirring, the product in THF solution was centrifuged and dried under vacuuming overnight. The XRD pattern of the product is showed in Fig. 2a, in which the peaks assigned to the (111), (200), (220) and (311) planes of Li_2S can be clearly observed. Fig. 2b exhibits the EDX mapping off the Li_2S/KB/CNT electrode obtained by the chemical pre-lithiaition process. From the element mapping of sulfur and carbon, the uniform distribution of Li_2S/KB composite on the cathode can be certified.

Li_2S/KB/C cathode was fabricated by the same pre-lithiation process on a flat carbon film on Al as a comparison sample to certify the influence of the 3D nano structured CNT film. In order to identify the product in the S/KB electrodes after chemical reaction with Li^+Naph^- at room temperature, the electrode of Li_2S/KB/CNT and Li_2S/KB/C were analyzed by XPS. Fig. 3 presents the S 2p peaks which split to S $2p_{3/2}$ and S $2p_{1/2}$ dual peaks with an area ratio around 2:1 causing by spin-orbit splitting. The lone dual peaks at high binding energies (167.1 eV) appeared in Fig. 3a and b is attributed to the sulfonate [35,36] formed by the sulfonation reaction between Li^+ and trace amount of oxygen and water in the glovebox during the long-time storage after fabrication. The S $2p_{3/2}$ peaks located at the low binding energy region (160–164 eV) are assigned to sulfides [37]. There are two pairs of S $2p_{3/2}$ and S $2p_{1/2}$ dual peaks in the low binding energy region both in the Li_2S/KB/CNT sample (Fig. 3a) and Li_2S/KB/C sample (Fig. 3b). Both of them exhibit the peak centered at 160.5 eV. With referring to the XRD results in Fig. 2b, it can be confirmed that the peak located at 160.5 eV comes from the Li_2S [37,38]. The peak located at 162.5 eV (Li_2S/KB/CNT) and the peak at 161.9 eV (Li_2S_x/KB/C) can be assigned to Li_2S_x ($2 < x < 8$) [37], which is partly reduced compounds of S. The peak located at 164.1 eV which is attributed to sulfur substance in the Li_2S/KB/C sample can be observed. It is at the same position with the S $2p_{3/2}$ peak in S/KB electrode (Fig. 3c). It can be certified that some part of the S substance in the S/KB composite totally hasn't been involved in the reducing reaction with Li^+Naph^-. In order to clarify the exact reaction product of the two samples, it is necessary to calculate the atom ratio of different compounds.

As we know that the atom ratio can be calculated by empirical atomic sensitivity factors method in the following equation [39].

$$\frac{n_1}{n_2} = \frac{I_1}{S_1} \Big/ \frac{I_2}{S_2} \quad (2)$$

In this equation, 'n_1/n_2' represents atom ratio of peak 1 and peak 2, 'S' represents the atomic sensitivity factor of each element. Since both of the elements are sulfur, so $S_1 = S_2$. 'I' represents the amounts of peak area. The peak area can be obtained from Casa XPS software. The atom ratio of S related to different sulfide composition is calculated due to equation (2). The composition of the Li_2S/KB/CNT

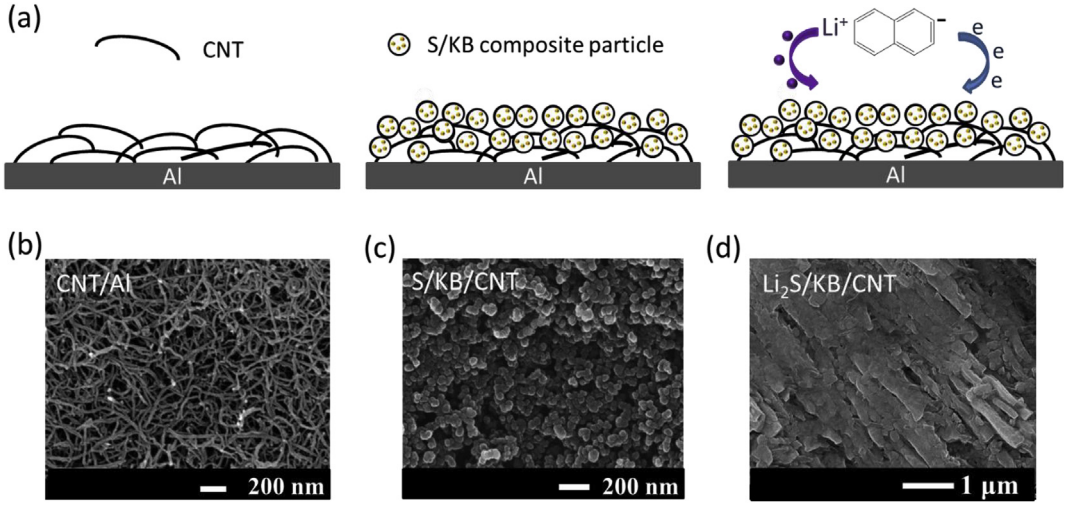

Fig. 1. (a) Schematic diagram of the fabrication process of Li_2S/KB/CNT electrode. SEM image of the surface on (b) CNT layer on Al foil (CNT/Al), (c) S/KB composite on CNT/Al substrate (S/KB/CNT), (d) Li_2S/KB/CNT electrode fabricated by chemical reaction.

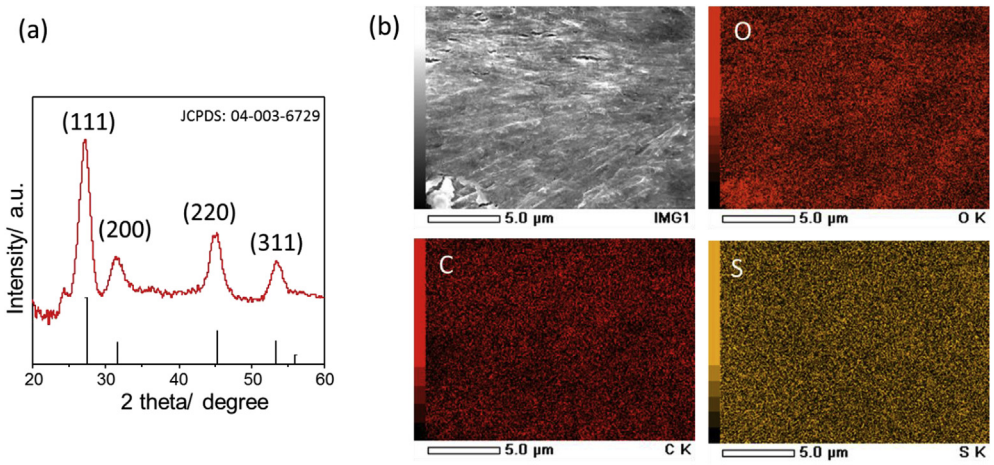

Fig. 2. (a) XRD pattern of the Li_2S particles fabricated by chemical reaction. (b) EDX mapping of the oxygen, carbon and sulfur elements on Li_2S/KB/CNT electrode fabricated by chemical reaction.

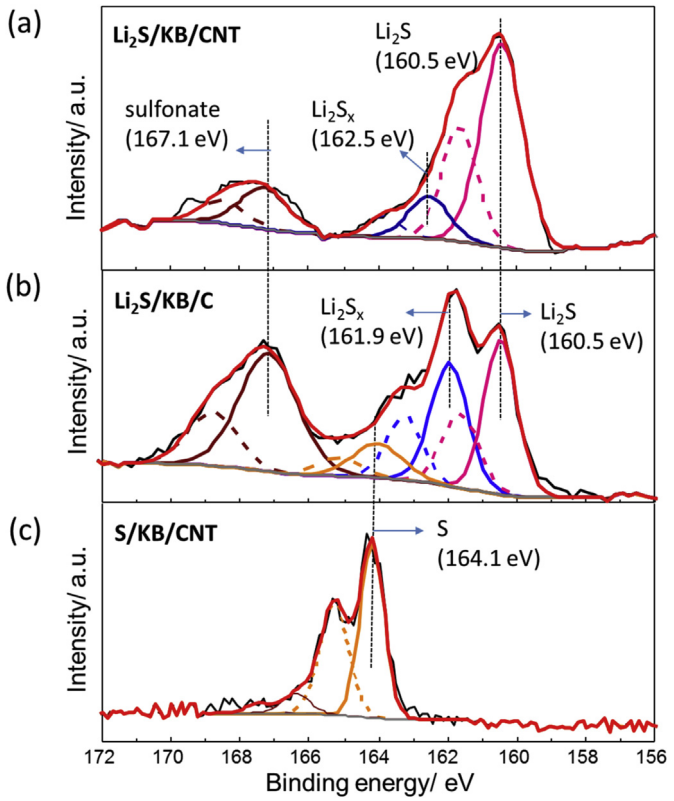

Fig. 3. XPS spectra of S 2p obtained on the (a) Li_2S/KB/CNT electrode fabricated by the chemical reaction with Li^+Naph^- at room temperature, (b) Li_2S/KB/C electrode fabricated by the chemical reaction with Li^+Naph^- at room temperature, (c) S/KB/CNT electrode.

electrode fabricated by chemical pre-lithiation are shown in Table 1. About 83.8% of the product is Li_2S and only 16.2% is polysulfides in the Li_2S/KB/CNT electrode. While in the Li_2S/KB/C electrode, only 45.2% of the sulfides is Li_2S, 39.6% is Li_2S_x and the last 15.2% remains S. The XPS results of the sulfur composite contents in each cathode indicated the pre-lithiation depth of the electrodes prepared by the chemical reaction with Li^+Naph^- at room temperature.

The Electrochemical performance of the Li_2S/KB/CNT and Li_2S/KB/C half cells prepared by the chemical reaction with Li^+Naph^- at room temperature was analyzed after paired with Li foil as anode.

Table 1
The S atom ratio of according to different sulfide compositions of the Li_2S/KB/CNT electrode and the Li_2S/KB/C electrode prepared by the chemical reaction with Li^+Naph^- at room temperature.

Sample	S (at.%) 164.1 eV	Li_2S_x (at.%) 161.9–162.5 eV	Li_2S (at.%) 160.5 eV
Li_2S/KB/CNT	0	16.2	83.8
Li_2S/KB/C	15.2	39.6	45.2

Since $LiNO_3$ will decompose under 1.8 V, the test window was controlled above 1.8 V [40]. In Fig. 4a, the cycling performance of the two cathodes was analyzed at 0.1 C-rate. It is remarkable to see that the in the first cycle, the coulombic efficiency of the Li_2S/KB/C cathode is much higher than 100% (~191%), which indicates the partly lithiated state of sulfur. Fig. 4b shows the 1st cycle of CV curve of the two Li_2S cathodes. In the case of Li_2S/KB/C cathode, the value of initial open-circuit voltage (OCV, 2.1 V vs Li/Li^+) can be ascribed to partial lithiation state of sulfur. While the OCV of Li_2S/KB/CNT is 2.0 V which indicated the fully lithiated state. The 1st anodic peak which according to the oxidization from Li_2S to S indicating the high charging capacity of Li_2S/KB/CNT cathode. Fig. 4c illustrates the first charge discharge curve of both cathodes, which are started from a de-lithiation process. It can be seen that the Li_2S/KB/C cathode showed low capacity of 474 mAh g^{-1}(sulfur), while the Li_2S/KB/CNT cathode showed high capacity of 1416 mAh g^{-1}(sulfur). In the first discharge curve, the Li_2S/KB/C cathode showed 987 mAhgg^{-1}(sulfur) capacity, which is about 400 mAh g^{-1} (sulfur) lower than that of Li_2S/KB/CNT cathode. The following cycling performance of both electrodes is exhibited in Fig. 4a. The capacity of Li_2S/KB/CNT cathode keeps 200 mAh g^{-1} (sulfur) higher than the Li_2S/KB/C cathode. Both of them exhibit stable Coulombic efficiency above 90% contributed by the KB served as physical confinement. Fig. 4d illustrate the CV curve from 1st cycle to 4th cycle of the Li_2S/KB/CNT cathode. Two cathodic peaks located at 2.29 V and 1.99 V are assigned to the reduction of S_8 to Li_2S_x and the reduction of Li_2S_4 to Li_2S respectively. The ambiguous two peaks at 2.34 V and 2.40 V from cycle 2 to cycle 4 correspond to the two-step transformation from Li_2S to Li_2S_x and from Li_2S_x to S_8 [41]. The relative good repeatability of the CV curves in the following cycles indicates the stable cycling performance of the Li_2S/KB/CNT cathode. Fig. 4e illustrates the charge discharge curve of Li_2S/KB/CNT in different cycles. It can be observed that in the 100th cycle, the discharge capacity is 567 mAh g^{-1} (sulfur), which is about 80% of the capacity in the 10th cycle.

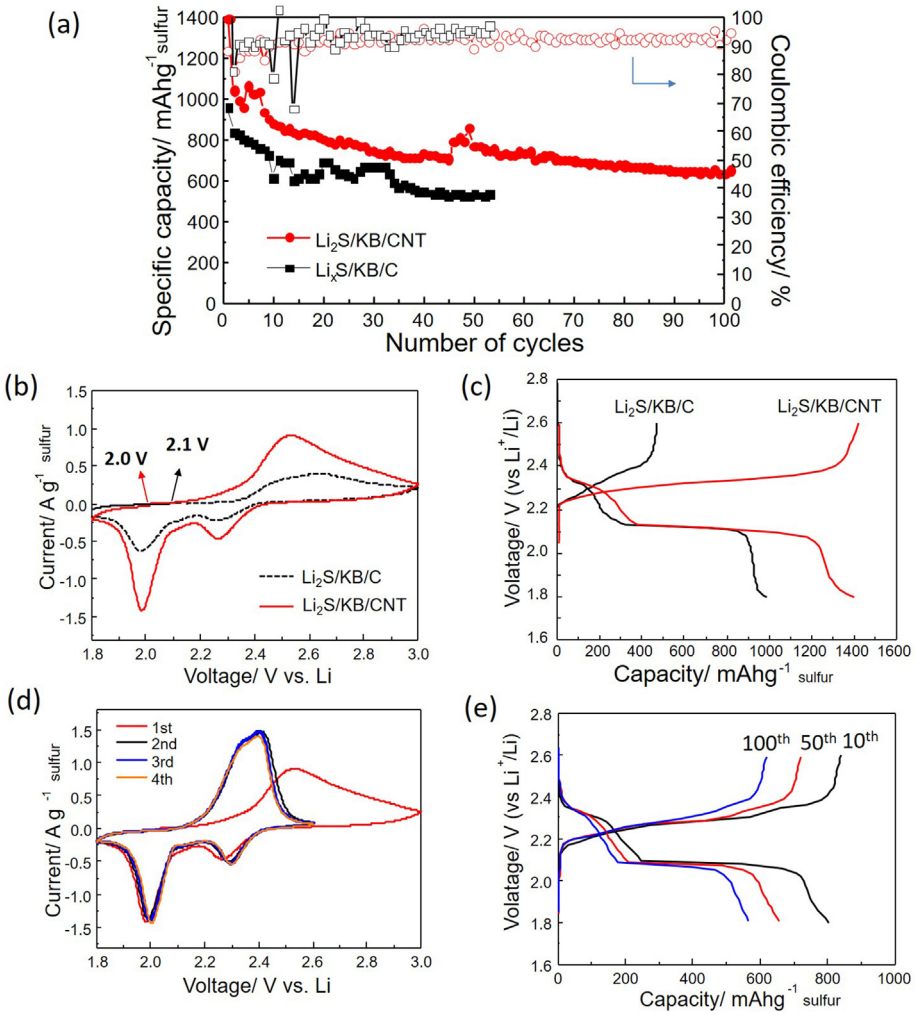

Fig. 4. (a) Cycling performance; (b) Cyclic voltammogram; (c) 1st charge discharge curves of the Li_2S/KB/CNT electrode and the Li_2S/KB/C electrode prepared by the chemical reaction with Li^+Naph^- at room temperature. (d) Cyclic voltammogram (e) Charge discharge curves of different cycles of the Li_2S/KB/CNT electrode.

The residual of sulfur substance in the Li_2S/KB/C cathode after chemical reaction is assumed to be caused by the insufficient contact between Li^+Naph^- and sulfur substance in the S/KB composite. In order to prove this hypothesis, we applied elevated temperature to accelerate the diffusion and reaction speed of the Li^+Naph^- solution. As we know that elevated temperature can increase the molecule's reactivity due to the basic theory of chemical reaction kinetics which contribute to accelerating the reaction rate. At the same time, the Li^+ ion transport in the S/KB solid is highly dependent on the kinetics of cation transport due to Fick's law. Thus, at a given ion concentration gradient, cation transport in a solid electrode is dependent on the temperature. At the temperature of 80 °C, which is still lower than the reaction temperature between the organolithium reagent and S reported [27,29], the cycling performance of the fabricated Li_2S/KB/C cathode is illustrated in Fig. 5a. Instead of the almost 200% Coulombic efficiency of Li_2S/KB/C at room temperature (Fig. 4c), the Li_2S/KB/C cathode obtained at 80 °C showed serious overcharged phenomenon in the 1st cycle. The low efficiency about 40% manifest that a large amount of polysulfides dissolved into the electrolyte in the first charging process. XPS analysis of the Li_2S/KB/C cathode obtained at 80 °C is shown in Fig. 5b. There is no peak arising from elemental sulfur can be observed in the S 2p curve, which certified the relatively fully lithiated state of S. From the discussion of the material analysis and electrochemical property of the Li_2S/KB/C cathode fabricated at elevated temperature, it is convictive to say that diffusion velocity is the main factor that cause the partial lithiation state of S/KB composite. The 3D nanostructured CNT layer facilitated chemical reaction between S/KB composites and Li^+Naph^- by acting as a 3D diffusion network for the Li^+Naph^- solution. As a result, the Li^+Naph^- solution can diffuse through the 3D nanotubes to contact with all the S/KB nanoparticles much easier. In the case of flat carbon layer, it is difficult for the Li^+Naph^- solution to diffuse through the S/KB layer. Inset image in Fig. 5a is the SEM image of the Li_2S/KB/C cathode obtained at 80 °C. Instead of the nano particle composed cathode surface, rough plate-like particles can be observed, indicating the destroyed S/KB composite structure of the cathode. The destroyed nano particle structure of Li_2S/KB/C cathode fabricated at high temperature is the main reason leading to the low capacity.

The cycling performance at various C-rates was taken place to evaluate the electrochemical behavior of the fabricated Li_2S/KB/CNT cathode. As illustrated in Fig. 6, the Li_2S/KB/CNT cathode showed stable cycling performance from 0.1 C-rate to 2 C-rate. It keeps high capacity around 500 mAh g^{-1} (sulfur) even at 2 C-rate. Then turn back to 0.1 C-rate, the discharge capacity is keep stable around 700 mAh g^{-1} (sulfur). Fig. 6b illustrates the charge discharge curve configuration at different C-rates of the Li_2S/KB/

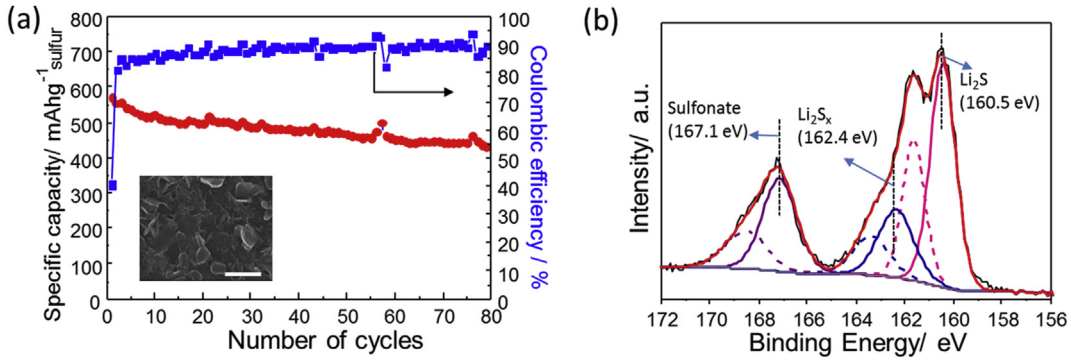

Fig. 5. (a) Cycling performance of the Li_2S/KB/C cathode fabricated by the chemical reaction with Li^+Naph^- at 80 °C. Inset is the SEM image of the electrode surface, the scale bar is 500 nm. (b) XPS spectra of S 2p obtained on Li_2S/KB/C fabricated by the chemical reaction with Li^+Naph^- at 80 °C.

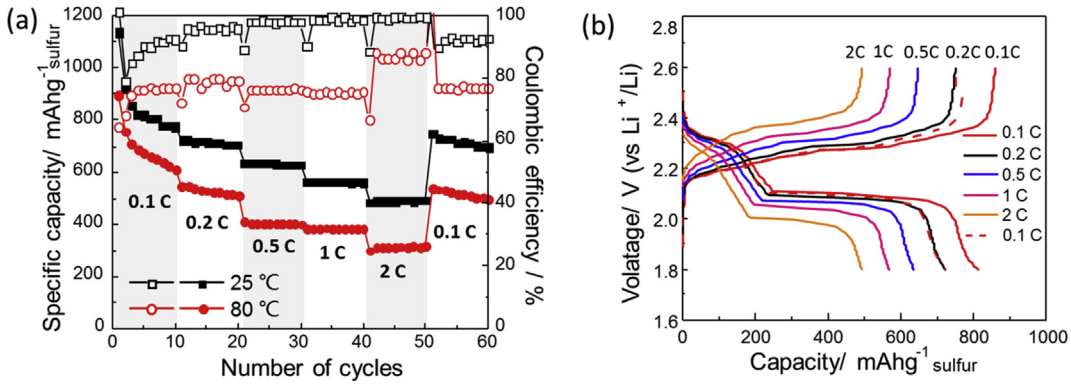

Fig. 6. (a) Cycling performance at various C-rates of Li_2S/KB/CNT electrodes fabricated by chemical reaction at 25 °C and at 80 °C respectively. (b) The typical charge discharge curves at various C-rates of the Li_2S/KB/CNT electrodes fabricated by chemical reaction at 25 °C.

CNT half cell. It is clear to see that the flat charge plateau and two step discharge plateau even at 2 C-rate.

For deeper study on the influence of the temperature (80 °C) on the cycling performance of the pre-lithiated cathode, 80 °C has been applied in the chemical fabrication of Li_2S/KB/CNT cathode. The cycling performance at various C-rates is illustrated in Fig. 6a to compare with the room temperature fabricated cathode. In the 1st cycle, the Coulombic efficiency decreased to 64% and the 1st discharge capacity decreased to 894 mAh g^{-1} (sulfur), which agrees with the low capacity and efficiency of the Li_2S/KB/C fabricated at 80 °C. It is convincing to conclude that chemical reaction between Li^+Naph^- solution and S/KB electrode can be accelerated by elevated temperature. But the broken of nano particle structure will lead to the slump of cycling performance.

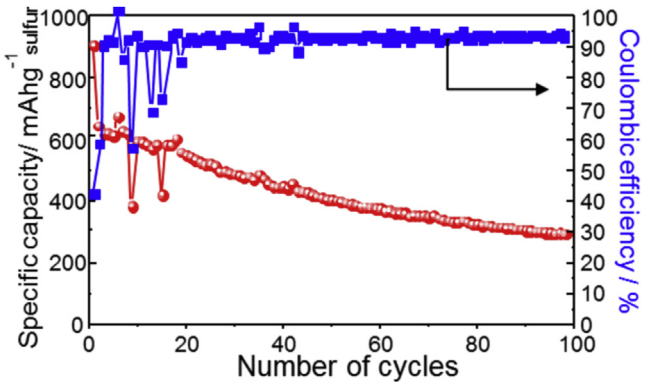

Fig. 7. Cycling performance at 0.1 C-rate of Li_2S/KB/CNT electrode fabricated by chemical reaction at room temperature without surface rinsing.

Since this on-site Li_2S fabrication method first realized at room temperature pre-lithiation, it is promising to realize the in-situ fabrication of Li_2S cathode in the S/KB cell configuration. No rinsing process was applied after chemical reaction on S/KB/CNT electrode. After dropping the carefully calculated amount of Li^+Naph^-, the Li_2S/KB/CNT was dried in the glovebox for a few hours and then was directly assembled into a coincell without rinsing. As a result, the reaction side product Naph will co-exist in the Li_2S/KB/CNT. In Fig. 7, there is fluctuation in the first few cycles, which is thought to be caused by the Li^+ ion interaction with the Naph residue. The low Coulombic efficiency and capacity loss in the first cycle is possible causing by the Li^+ ion reacted with Naph residue. In 9th cycle and 15th cycle, the capacity dropped again because of the influence of Naph. Since Li^+Naph^- cannot keep stable Li^+ ion intercalation and de-intercalation rock-chair reaction, after all the Naph became dead for Li^+ ion intercalation, the disrupting phenomenon during cycling disappeared. Though the capacity decreased to 600 mAh g^{-1} (2nd cycle), this experiment is meaningful for future study of in-situ pre-lithiation in a Li metal free full cell configuration.

4. Conclusion

In conclusion, a new chemical pre-lithiation method to fabricate Li_2S cathode has been realized at room temperature at first time by employing a 3D structured CNT interlayer. This chemical reaction was carried out by using the Li^+Naph^- organolithium as a reducing reagent. The 3D nanostructured CNT current collector provided the

3D diffusion path for facilitating the ion transportation. The fabricated Li_2S/KB/CNT cathode at room temperature showed stable cycling performance with a 600 mAh g^{-1} capacity after 100 cycles at 0.1 C-rate and high capacity of 500 mAh g^{-1} at 2 C-rate. We have demonstrated that the Li_2S cathode obtained after the on-site pre-lithiation can be assembled into battery without any further process. We believe this room temperature pre-lithiation method will make a little contribution for realizing pre-lithiation in future Li metal free battery.

Acknowledgement

This work is partly supported by Advanced Low Carbon Technology Research and Development Program Special Priority Research Area “Next-generation Rechargeable Battery” (ALCA-Spring) from the Japan Science and Technology Agency (JST), Japan. Y. W. would also like to express her gratitude to Japan Society for the Promotion of Science (JSPS) KAKENHI Grant Number JP17J09973.

References

[1] J.B. Goodenough, K.-S. Park, J. Am. Chem. Soc. 135 (2013) 1167–1176.
[2] P.G. Bruce, S.A. Freunberger, L.J. Hardwick, J.M. Tarascon, Nat. Mater. 11 (2012) 19–29.
[3] A. Manthiram, Y. Fu, S.H. Chung, C. Zu, Y.S. Su, Chem. Rev. 114 (2014) 11751–11787.
[4] S. Zhang, K. Ueno, K. Dokko, M. Watanabe, Adv. Energy Mater. 5 (2015), 1500117.
[5] X. Ji, K.T. Lee, L.F. Nazar, Nat. Mater. 8 (2009) 500–506.
[6] W. Li, G. Zheng, Y. Yang, Z.W. Seh, N. Liu, Y. Cui, Proc. Natl. Acad. Sci. 110 (2013) 7148–7153.
[7] Q. Pang, J. Tang, H. Huang, X. Liang, C. Hart, K.C. Tam, L.F. Nazar, Adv. Mater. 27 (2015) 6021–6028.
[8] Z. Lin, Z. Liu, W. Fu, N.J. Dudney, C. Liang, Adv. Funct. Mater. 23 (2013) 1064–1069.
[9] Y. Fu, Y.-S. Su, A. Manthiram, Adv. Energy Mater. 4 (2014), 1300655.
[10] T. Takeuchi, H. Sakaebe, H. Kageyama, H. Senoh, T. Sakai, K. Tatsumi, J. Power Sources 195 (2010) 2928–2934.
[11] T. Yamada, S. Ito, R. Omoda, T. Watanabe, Y. Aihara, M. Agostini, U. Ulissi, J. Hassoun, B. Scrosati, J. Electrochem. Soc. 162 (2015) A646–A651.
[12] M. Hagen, E. Quiroga-González, S. Dörfler, G. Fahrer, J. Tübke, M.J. Hoffmann, H. Althues, R. Speck, M. Krampfert, S. Kaskel, H. Föll, J. Power Sources 248 (2014) 1058–1066.
[13] Y. Son, J.-S. Lee, Y. Son, J.-H. Jang, J. Cho, Adv. Energy Mater. 5 (2015), 1500110.
[14] Y. Yang, G. Zheng, S. Misra, J. Nelson, M.F. Toney, Y. Cui, J. Am. Chem. Soc. 134 (2012) 15387–15394.
[15] F. Ye, M. Liu, X. Zhang, W. Li, Z. Pan, H. Li, S. Zhang, Y. Zhang, Small 12 (2016) 6.
[16] K. Cai, M.K. Song, E.J. Cairns, Y. Zhang, Nano Lett. 12 (2012) 6474–6479.
[17] L. Chen, Y. Liu, M. Ashuri, C. Liu, L.L. Shaw, J. Mater. Chem. A 2 (2014) 18026–18032.
[18] J. Liu, H. Nara, T. Yokoshima, T. Momma, T. Osaka, J. Power Sources 273 (2015) 1136–1141.
[19] F. Wu, H. Kim, A. Magasinski, J.T. Lee, H.-T. Lin, G. Yushin, Adv. Energy Mater. 4 (2014), 1400196.
[20] F. Wu, J.T. Lee, E. Zhao, B. Zhang, G. Yushin, ACS Nano 10 (2016) 1333–1340.
[21] M. Wu, Y. Cui, Y. Fu, ACS Appl. Mater. interfaces 7 (2015) 21479–21486.
[22] K. Zhang, L. Wang, Z. Hu, F. Cheng, J. Chen, Sci. Rep. 4 (2014) 6467.
[23] M. Kohl, J. Brückner, I. Bauer, H. Althues, S. Kaskel, J. Mater. Chem. A 3 (2015) 16307–16312.
[24] J. Liu, H. Nara, T. Yokoshima, T. Momma, T. Osaka, Electrochimica Acta 183 (2015) 70–77.
[25] Z. Yang, J. Guo, S.K. Das, Y. Yu, Z. Zhou, H.D. Abruña, L.A. Archer, J. Mater. Chem. A 1 (2013) 1433–1440.
[26] K. Han, J. Shen, C.M. Hayner, H. Ye, M.C. Kung, H.H. Kung, J. Power Sources 251 (2014) 331–337.
[27] Y. Yang, M.T. McDowell, A. Jackson, J.J. Cha, S.S. Hong, Y. Cui, Nano Lett. 10 (2010) 1486–1491.
[28] Y. Hwa, J. Zhao, E.J. Cairns, Nano Lett. 15 (2015) 3479–3486.
[29] C. Nan, Z. Lin, H. Liao, M.K. Song, Y. Li, E.J. Cairns, J. Am. Chem. Soc. 136 (2014) 4659–4663.
[30] X. Li, C.A. Wolden, C. Ban, Y. Yang, ACS Appl. Mater. interfaces 7 (2015) 28444–28451.
[31] S. Ahn, M. Jeong, T. Yokoshima, H. Nara, T. Momma, T. Osaka, J. Power Sources 336 (2016) 203–211.
[32] J.-W. Gao, Synlett 2012 (02) (2012) 317–318.
[33] G. Wu, M. Huang, Chem. Rev. 106 (2006) 2596–2616.
[34] Y. Wu, T. Yokoshima, H. Nara, T. Momma, T. Osaka, J. Power Sources 342 (2017) 537–545.
[35] M.J. Tarlov, D.R. Burgess Jr., G. Gillen, J. Am. Chem. Soc. 115 (1993) 5305–5306.
[36] J.A. Rodriguez, T. Jirsak, A. Freitag, J.C. Hanson, J.Z. Larese, S. Chaturvedi, Catal. Lett. 62 (1999) 113–119.
[37] Y. Fu, C. Zu, A. Manthiram, J. Am. Chem. Soc. 135 (2013) 18044–18047.
[38] Y. Fu, Y.S. Su, A. Manthiram, Angew. Chem. 52 (2013) 6930–6935.
[39] C.D. Wagner, L.E. Davis, M.V. Zeller, J.A. Taylor, R.H. Raymond, L.H. Gale, Surf. Interface Analysis 3 (5) (1981) 211–225.
[40] S.S. Zhang, Electrochimica Acta 70 (2012) 344–348.
[41] M. Wild, L. O'Neill, T. Zhang, R. Purkayastha, G. Minton, M. Marinescu, G.J. Offer, Energy Environ. Sci. 8 (2015) 14.